https://dx.doi.org/10.1016/j.scitotenv.2019.134069

Comparison of $PM_{2.5}$ pollution between an African city and an Asian metropolis

Lewei Zeng[1], Francis Offor[1], Lingxi Zhan[1,2], Xiaopu Lyu[1], Zhirong Liang[1], Luyao Zhang[1], Jiaying Wang[1], Hairong Cheng[2], Hai Guo[1,*]

[1] Air Quality Studies, Department of Civil and Environmental Engineering, The Hong Kong Polytechnic University, Hong Kong, China

[2] Department of Environmental Science and Engineering, School of Resource and Environmental Sciences, Wuhan University, Wuhan, China

Abstract

Fine particulate matter ($PM_{2.5}$) samples were collected simultaneously at urban sites in Lagos (ULG site) and in Hong Kong (TC site) for four consecutive weeks in July and August, 2017, in order to investigate the potential to apply successful pollution control measures from HK to Lagos. To compare chemical characteristics and sources of $PM_{2.5}$ in these two regions for the first time, organic carbon (OC), elemental carbon (EC), water soluble ions (WSIs), and elements were analyzed. It was found that total carbon and elements were much abundant ($p<0.05$) at ULG, indicating more severe $PM_{2.5}$ pollutions in Lagos, while levels of WSIs were comparable ($p=0.05$) at both sites. Higher correlation coefficient (0.79) between OC and EC but lower OC/EC ratio (1.81±0.18) at ULG (TC: 0.48; 3.51±0.60) revealed the dominant role of primary sources in Lagos. Furthermore, examination of secondary organic carbon (SOC)/OC ratio implied that only 12±8% of OC were attributable to secondary organic formation at ULG whereas 47±9% at TC. Positive matrix factorization (PMF) model resolved six $PM_{2.5}$ sources at each site, in which vehicular emissions contributed the most (32.2±3.18%) at ULG, while secondary inorganic aerosols (including secondary SO_4^{2-} and NO_3^-) together with regional biomass burning (36.5±5.21%) dominated at TC. Sea salt sources were significant at both harbor cities. For inter-comparison, the sum of vehicular emission and fugitive dust accounted for ~40.9% at ULG, and was triple that at TC ($p<0.01$) in concentration. Severer primary sources of $PM_{2.5}$, especially from the street-level pollution in Lagos called for effective control measures, such as periodical upgrade of fuel and retrofits on vehicles, which have been successfully promoted in Hong Kong and were worth learning from.

Keywords: Nigeria; Hong Kong; WSI; Element; Source apportionment

*Corresponding author. ceguohai@polyu.edu.hk (Prof. H. Guo)

1. Introduction

Airborne fine particulate matter ($PM_{2.5}$) has caused worldwide concerns because of its detrimental effects on human health, atmospheric visibility, and global climate change (Seinfeld and Pandis, 1998; Cheung et al., 2005; Anton et al., 2010; Fiore et al., 2012). Although many studies on the chemical characteristics, sources and toxicity of $PM_{2.5}$ have been conducted in North America, Europe and Asia (Cooke et al., 2007; Crouse et al., 2012; Krall et al., 2017; Song et al., 2017; Wang et al., 2017; Samek et al., 2018), a handful of references were available in Africa. Moreover, ambient air quality standards of $PM_{2.5}$ have been well established in the United States, the European Union, China and other countries (EEA, 2017; AUDEE, 2018; PRCMEE, 2018; USEPA, 2018), while no such regulatory document exists in Africa including Nigeria (Offor et al., 2016). As studies have reported severe $PM_{2.5}$ pollution and numerous diseases related to $PM_{2.5}$ in Africa (Petkova et al., 2013; Zhou et al., 2014; Gumede and Savage, 2017), the lack of local $PM_{2.5}$ standards hinders the control of air pollution in this region.

To better understand the $PM_{2.5}$ pollution in Africa and learn from the successful experience in $PM_{2.5}$ control from developed countries, Lagos in Nigeria and Hong Kong in China were chosen for comparative study of $PM_{2.5}$ pollution. Lagos is a developing city on the southwestern coast of Nigeria, which is characterized by a tropical wet and humid climate and typically divided into the dry season (winter, November to March) and the rainy season (summer, April to October) (Adelekan, 2009). Hong Kong is a developed city on the southern coast of China, characterized by a subtropical climate under the influence of the East Asian Monsoon (Ho et al., 2006). Both Lagos and Hong Kong are port cities subjected to the typical air pollution in coastal regions of Africa and Asia, respectively. However, because of the different population density, economic situations and industrial structures between Lagos and Hong Kong (Ferguson et al., 2000; Adelekan, 2009; GovHK, 2019), the characteristics of $PM_{2.5}$ pollution in these two cities are expected to be specific.

Lagos, the biggest city of Nigeria, has possessed about 70% of the nation's industrial and commercial activities (Makinde, 2005; Olowoporoku, 2007). Emissions from road traffic, industries, ships and unpaved roads significantly contribute to the $PM_{2.5}$ load due to accelerated urbanization and industrialization (Offor et al., 2016; Orogade et al., 2016). Furthermore, increasing drought episodes and savannah fires/biomass

burning are also main contributors of mineral dusts and carbonaceous aerosols in $PM_{2.5}$ (Owoade et al., 2013). The lack of air quality monitoring in Nigeria causes a poor perception of airborne particulate characteristics (Petkova et al., 2013), leading to the absence of effective strategies upon PM mitigation.

Hong Kong is a metropolis with high density of population and vehicles. Many $PM_{2.5}$ studies have been carried out in the past decades. Chemical characteristics of $PM_{2.5}$ at different sites implied that the major components were organic matter in urban area and sulfate in rural area (Ho et al., 2006). Similar result was found at a suburban site with sulfate being the most predominant substance, followed by ammonium components (Huang et al., 2014). The main $PM_{2.5}$ sources were vehicular emissions, secondary sulfate and nitrate, residual oil combustion (ship emission), sea salt, crustal dust and solvent usage (Guo et al., 2009a; Huang et al., 2014; Cheng et al., 2015). In order to mitigate the PM pollution, a series of control measures have been adopted by the Hong Kong government during the last decade. For instance, the Euro V standard was enforced in Hong Kong in 2010 to tighten the vehicular emissions (So et al., 2007; Yuan et al., 2013).

Study that spanned the Indian Ocean was conducted simultaneously in Africa and Asia is rare. Compared to inland regions, sea salt is a vital source of $PM_{2.5}$ in coastal areas (Zhang et al., 2014; Wang et al., 2018). Even so, knowledge gaps exist about similarities and differences in chemical compositions and sources of $PM_{2.5}$ between Lagos and Hong Kong, which hamper the direct application of Hong Kong's air pollution control strategies in Africa. Thus, in this study, simultaneous measurements of $PM_{2.5}$ in Lagos and Hong Kong were conducted to investigate the chemical compositions and sources of $PM_{2.5}$ as well as understand the differences and similarities of $PM_{2.5}$ pollution in two cities. This study laid a solid foundation for the promotion of effective control measures of Hong Kong in Lagos, facilitating the technology/mitigation policies transfer from developed region to developing region.

2. Materials and methods

2.1. Sampling

$PM_{2.5}$ sampling was conducted simultaneously at the University of Lagos (ULG), Lagos and Tung Chung (TC), Hong Kong, for 4 consecutive weeks (13 July - 10 August, 2017) in summer in Hong Kong and rainy (summer) season in Lagos (Fig. 1). In Lagos, the

field measurement was conducted on the rooftop of a 3 storey building (6.52°N, 3.39°E, 14.6 m a.s.l.) inside the Faculty of Science Complex of ULG. The site was considered as an urban site mixed with residential, commercial and industrial activities. The campus was about 1.4 km away from the Lagos lagoon. The sampling site in Hong Kong was on the rooftop of a primary school building (22.3°N, 113.93°E, 27 m a.s.l.) in Tung Chung, northern Lantau Island. The site was a residential site with many residential and some commercial activities, as well as highways and railway lines around. Detailed description was provided in (Guo et al., 2009b). During the sampling period, marine air masses prevailed at both sites (Fig. S1), implying the dominance of local effects on the $PM_{2.5}$ pollution.

Fig. 1 Location of sampling sites in Lagos (ULG) and in Hong Kong (TC).

$PM_{2.5}$ samples were collected onto 8×10" quartz fiber filters (QFF) (Whatman, QM-A) for 24 hrs using high volume samplers in Hong Kong (Anderson Instruments Inc., Model G1200-2.5, flow rate: 700 L/min) and Lagos (Shanghai X-Trust Analytical Instruments Co., Model XT-1025, flow rate: 1000 L/min). A total of 59 (Lagos: 29 filters; Hong Kong: 30 filters) samples were obtained during the whole sampling campaign. Prior to sample collection, the QFFs were baked in an oven for 6-h at 500°C to remove organic contaminants, then packed in aluminum foil, sealed in bags and stored in a freezer at -20°C. Before and after sampling, all filters were equilibrated in humidity (35-45% relative humidity) and temperature (25°C) controlled windowless room for 24 hours by Sartorius LA130S-F Filter Balance. Blank filters were collected strictly followed the aforementioned procedures in order to remove the impact of positive/negative artefacts during the sampling as well as the measurements. Since

quartz filters were known to readily loose fibers which could significantly affect their mass, these filters were not used for $PM_{2.5}$ mass measurements in this study.

Meteorological parameters at ULG were obtained from the Nigerian Meteorological Agency (NIMEA) forecast station at Lagos Marine (representative of ULG site), while the weather data at TC were measured using a mini weather station (Vantage Pro2TM, Davis Instruments Corp., USA). The meteorological parameters measured included relative humidity, temperature, solar radiation intensity and wind speed/direction. In addition, data of trace gases at TC were obtained from the Hong Kong Environmental Protection Department (HKEPD). During the sampling period, the average relative humidity, temperature and wind speed were 85.7%, 26.4°C and 7.48 m/s at ULG, and 81.9%, 29.4°C and 0.92 m/s at TC.

2.2. Chemical Analysis

The elemental carbon (EC) and organic carbon (OC) in $PM_{2.5}$ were analyzed using a Thermal/Optical Carbon Analyzer (DRI Model 2001). The carbon that evolved at each temperature was oxidized to carbon dioxide (CO_2), followed by the reduction to methane (CH_4), then quantified with a flame ionization detector. A 0.526 cm^2 punch aliquot of a sample quartz filter was stepwise heated at temperatures of 120°C (OC1), 250°C (OC2), 450°C (OC3), and 550°C (OC4) in a non-oxidizing helium (He) atmosphere, and 550°C (EC1), 700°C (EC2), and 800°C (EC3) in an oxidizing atmosphere of 2% oxygen in a balance of helium.

Before instrumental analysis of water-soluble ions (WSIs), one-quarter of a filter was put into a glass tube and 25 mL deionized water (18.2 ΩM cm^{-1}) was then added. After 45-min ultrasonic extraction, the solution was filtered through an acetate-cellulose filter with 0.45 μm pore size. Concentrations of the WSIs in the aqueous extract, including four anions (Cl^-, Br^-, NO_3^- and SO_4^{2-}) and five cations (Na^+, NH_4^+, K^+, Mg^{2+} and Ca^{2+}), were measured by an Ion Chromatograph (Dionex Integrion HPIC System).

Another quarter of a filter was placed in a Teflon vessel, digested with a 10 mL mixture of HNO_3-HCl (1:1, v/v) in a microwave system (XT-9900A, Shanghai Xintuo Co.) for 45 min. After the digested solution cooled down to room temperature, it was filtered through a 0.45 μm acetate cellulose filter. The filtrate was then diluted using deionized water to 50 mL, and a combination of both Inductively Coupled Plasma Mass Spectrometry (Spectroblue FMX36) and Inductively Coupled Plasma-Optical Emission

Spectrometry (Agilent 720) was used to determine the concentrations of 23 trace elements (Ag, Al, As, Ba, Be, Ca, Cd, Co, Cr, Cu, Fe, K, Mg, Mn, Mo, Na, Ni, Pb, Sb, Se, Sn, V and Zn).

2.3. Quality Assurance and quality control

Analyses of blank samples from sampling site and in the laboratory were performed using the same methods as above. All the carbonaceous components, WSIs and elements data were corrected by the field blank. When particulate OC was collected on the quartz filter, positive artifacts would be caused by the absorption of semi-volatile organic vapors on the quartz filter media, whereas negative artifacts generated during the evaporation of semi-volatile OC on the filter. Previous studies (Kim et al., 2001; Mader et al., 2003; Subramanian et al., 2004; Park et al., 2006) conducted in urban environment demonstrated 1.64-18.3% positive artifacts in quartz filter. Besides, Subramanian et al. (2004) reported negative artifacts less than 10%. To conclude, it can be considered that the sampling of OC on quartz filters would have around 10% positive artifacts.

During the OC/EC measurement, the analyzer was calibrated with CH_4 standard every day. The repeatability and method detection limits (MDLs) for the carbonaceous components were 10% and 0.01 $\mu g/m^3$. As for element analysis, mixed standards were injected every ten samples for calibration. The recovery efficiencies were between 83.8-102%, except for Al, K, Na (55.0-64.2%). Relative standard deviations for all samples were within 10% and MDL was 0.001 pg/m^3 for the elements. Besides, MDL for the WSIs 0.001 $\mu g/m^3$. Ions balance was used to ensure the quality of cations/anions analysis. Nano-equivalents of cations and anions derived from mass concentrations and molecular weights were performed as follows:

Cation equivalents ($nmol/m^3$)

$$= (NH_4^+/18 + 2 \times Ca^{2+}/40 + 2 \times Mg^{2+}/24 + K^+/39 + Na^+/23) \times 1000 \quad (1)$$

Anion equivalents ($nmol/m^3$)

$$= (Cl^-/35.5 + Br^-/79.9 + NO_3^-/62 + 2 \times SO_4^{2-}/96) \times 1000 \quad (2)$$

Significant linear correlations between cations and anions were observed at both ULG and TC with R^2 values of 0.90 and 0.99, respectively (Fig. 2). The slope of anions versus cations at ULG was slightly less than 1.0, implying some missing anions, which could

be carbonate or organic acid anions, e.g. acetate, oxalate and formate. However, the slope at TC was close to 1.0, indicating the well balance of the investigated ions (Fu et al., 2014).

In this study, the concentrations of ions and elements did not agree well with each other at both sites (R^2=0.11~0.61, as shown in Fig. S2). The element concentrations exceeded ions concentrations (except Ca), because not only soluble part, but also the non-soluble part were counted in the element levels. Moreover, due to the dissolution of elements originally on the quartz filters during the acid digestion, which led to an overestimation of measured element concentrations, ions (*i.e.* Na^+, K^+, Mg^{2+}) were selected as tracers in PMF instead of elements for better source quantification.

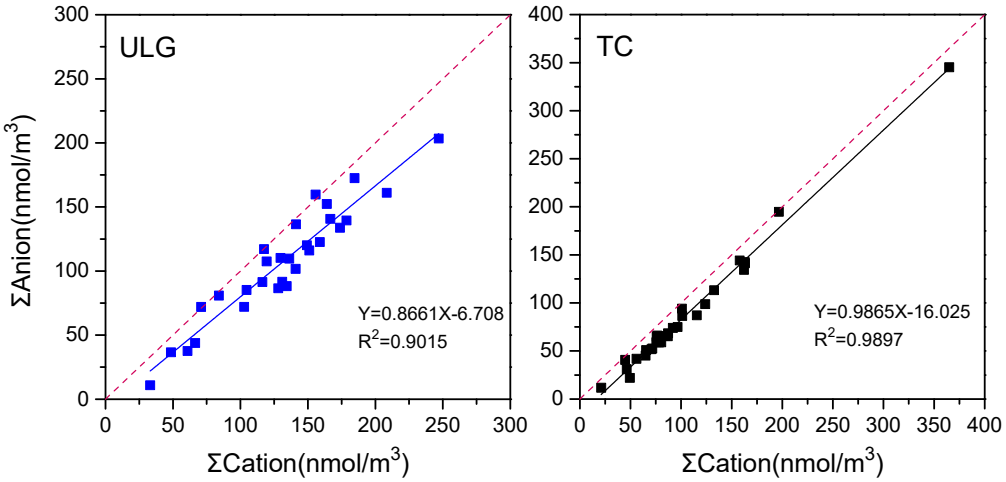

Fig. 2 Charge balance between cations and anions in $PM_{2.5}$ at ULG and TC. Red dotted lines represent one-to-one ratio.

2.4. Positive matrix factorization (PMF) model

The PMF receptor model (EPA v 5.0) has been broadly used for sources identification and quantification in PM pollution research (Huang et al., 2014; Lyu et al., 2016). It is a mathematical model that can reduce the amounts of variables to interpretative source types using multivariate factor analysis by decomposing the observed data by two matrices: factor profiles (F) and factor contribution (G), as shown in *E.q.* (3). The source number (p) is obtained by solving the following equation on the basis of the constraint that negative values are not allowed as the inputs.

$$X_{ij} = \sum_{k=1}^{p} g_{ik} f_{kj} + e_{ij} \quad (3)$$

In this equation, x_{ij} is the concentration of the j^{th} composition in the i^{th} sample, g_{ik} denotes the proportion of the k^{th} source to i^{th} sample, f_{kj} represents the fraction of the j^{th} composition in the k^{th} source, and e_{ij} is the residual value for the j^{th} composition in the i^{th} sample. p stands for the total number of independent source types. In order to evaluate the robust of the model results, a criterion of Q value is needed to be considered:

$$Q = \sum_{i=1}^{n} \sum_{j=1}^{m} \left[\frac{x_{ij} - \sum_{k=1}^{p} g_{ik} f_{kj}}{u_{ij}} \right]^2 \quad (4)$$

where m and n are the number of compositions and samples, while u_{ij} represents the uncertainty of the j^{th} components in the i^{th} sample. A lower Q value typically represents a robustness of the model-derived source apportionment. The daily average concentrations of 19 major $PM_{2.5}$ chemical compositions, including OC, EC, 7 species of WSIs and 10 element components, were selected for the model simulations (Text S1 describes the selection criteria). All selected components were of high abundance or being typical tracers of $PM_{2.5}$ sources at two sites (Lyu et al., 2016). WSIs were chosen as tracers prior to elements, on account of the possible overestimation of element concentrations. It should be noted that values below the detection limit (DL) were replaced by DL/2. The uncertainties applied for the samples of over the DL were $\sqrt{(10\%\text{concentration})^2 + \text{DL}^2}$, while 5/6 DL were adopted for those less than DL. In total, 28 and 30 samples were valid for the source apportionment analysis at ULG and TC, respectively. To increase the reliability of the model simulation, all 58 samples with 19 major chemical species were input into the model for simulation (Henry et al., 1984; Hu et al., 2010). The model was run for 20 times with a random seed, where the optimum solution was derived. Text S2 describes the rationality of sample number and diagnostics outputs of the results. Source profiles and contributions at ULG and TC were extracted separately from the output. Bootstrap method was run to quantify the uncertainty of all results.

3. Results and discussion

3.1. Concentrations of chemical components in $PM_{2.5}$

Table 1 presents the mean concentration with 95% confidence interval (CI), the minimum and maximum values of $PM_{2.5}$ including OC and EC, WSIs, and the eight major elements at ULG and TC. Fig. 3 displays the daily variations of the target components of $PM_{2.5}$ and the average fractions of WSIs at both sampling sites.

At ULG, the average OC and EC concentrations were 6.16±0.64 and 3.72±0.64 μg/m^3, respectively. Compared to the values reported in dry season in Cameroon, Africa (OC: 11.8-31.1 μg/m^3; EC: 2.60-5.90 μg/m^3), the OC value was lower while the EC level was within the range (Antonel and Chowdhury, 2014). At TC, the average OC and EC concentrations were 2.58±0.45 and 0.84±0.15 μg/m^3, respectively, consistent with the summer levels found in Hong Kong (OC: 1.49-7.96 μg/m^3; EC: 0.42-6.12 μg/m^3) (Ho et al., 2006). By comparison, the sum of OC and EC at ULG (9.88±1.19 μg/m^3) was approximately triple that at TC (3.42±0.54 μg/m^3) (p<0.001), implying larger fraction of carbonaceous species in $PM_{2.5}$ at ULG.

The total concentrations of WSIs were comparable at ULG (7.80±1.09 μg/m^3) and at TC (6.18±1.54 μg/m^3) (p=0.05) (Table 1). The secondary-formed SO_4^{2-} was the most abundant ion (anion), with the average of 2.50±0.20 and 3.16±0.72 μg/m^3 at ULG and TC, respectively, accounting for 31% and 48% of the total WSIs, respectively (see the pie charts in Fig. 3). In Lagos, motor vehicles, industrial activities and various combustion processes (*e.g.* waste combustion, biomass burning and thermal plant combustion) could emit high levels of SO_2 which was subsequently oxidized into SO_4^{2-} in the atmosphere (Sonibare and Jimoda, 2009). In Hong Kong, the SO_4^{2-} level found in this study was consistent with that in previous studies (1.69-4.7 μg/m^3) (Ho et al., 2006). Fig. S3 displays daily SO_4^{2-} together with wind speed/direction at TC. On the days with high SO_4^{2-} levels, sometimes (July 5 and 31) southwest/southeast winds dominated without any north winds, sometimes (July 26 and 28) northerly wind was observed, suggesting patial contribution of regional transport from inland China to local SO_4^{2-}. Similar phenomenon was also found in K^+, which was a typical tracer of biomass burning. In addition to regional transport, residual oil used as fuel in marine vessels contained sulfur contents up to 4.5% in Hong Kong (Yuan et al., 2013), which might be responsible for the abundant SO_4^{2-} observed at TC. As for cation, Na^+ had the highest concentration at both ULG (1.41±0.19 μg/m^3) and TC (0.92±0.24 μg/m^3). Higher Na^+ and Cl^- (major components of sea salt) were observed at ULG (p<0.001) and the sum of Na^+ and Cl^- explained ~35% of total WSIs at ULG and ~20% at TC, indicating a possible higher contribution of sea salt at ULG. Moreover, higher K^+ at ULG (p<0.001) implied severer biomass burning in Lagos since related activities were banned in Hong Kong. In addition, the summed concentration of NH_4^+, NO_3^- and SO_4^{2-} accounted for 50% and 69% of the total WSIs at ULG and TC, respectively, revealing the important

273 role of secondary formation in $PM_{2.5}$, expecially at TC.

274 Among the 23 elements, Na, Ca, Al, K, Fe and Mg were the most dominant
275 compositions, accounting for 90% and 95% of the total elements at ULG and TC. Na
276 was the most abundant element at two sites, with average values of 3,810±417 ng/m^3 at
277 ULG and 2,947±480 ng/m^3 at TC, contributing to 61% and 74% of overall element
278 components, respectively. Some elements at ULG had comparable levels to those
279 reported in Lagos (*i.e.* K: 850, Zn: 603.49, V: 9 ng/m^3) (Owoade et al., 2013), and
280 several elements at TC were also consistent with the previous studies in Hong Kong
281 (*i.e.* Zn: 103.28, V: 11.83 ng/m^3) (Ho et al., 2006). In the intercomparison of two sites,
282 K, Zn, Pb, Mn and Cd had much higher levels at ULG (p<0.05) (Table 1), while V and
283 Ni were more abundant at TC (p<0.01) (Table 1). Much lower Pb at TC was due to the
284 elimination of Pb-containing fossil fuel in Hong Kong. The results implied different
285 source profiles/contributions of $PM_{2.5}$ compositions between ULG and TC, which were
286 further studied in section 3.3.

287 **Table 1** Average concentrations of OC and EC, WSIs, and eight selected elements in
288 $PM_{2.5}$ at ULG and TC. The units of OC, EC and WSIs are μg/m^3, while it is ng/m^3 for
289 the elements.

	ULG				TC			
	Average	95%CI[4]	Min.	Max.	Average	95%CI[4]	Min.	Max.
OC	6.16	0.64	2.88	9.75	2.58	0.45	1.37	7.35
EC	3.72	0.64	1.49	9.51	0.84	0.15	0.38	1.93
ΣTotal carbon[1]	9.88	1.19	4.37	18.9	3.42	0.54	1.88	9.28
SO_4^{2-}	2.50	0.29	0.77	4.23	3.16	0.72	0.02	9.28
NO_3^-	1.07	0.20	0.31	2.63	0.53	0.32	0.05	4.28
NH_4^+	0.41	0.09	0.01	0.90	0.84	0.20	0.10	2.44
Cl^-	1.41	0.30	0.17	3.47	0.54	0.00	0.02	4.81
Na^+	1.41	0.19	0.47	2.24	0.92	0.24	0.13	3.83
K^+	0.47	0.06	0.06	0.73	0.10	0.03	0.02	0.42
Mg^{2+}	0.11	0.02	0.01	0.21	0.05	0.02	0.01	0.36
Ca^{2+}	0.57	0.12	0.18	1.59	0.38	0.22	0.05	3.15
ΣWSIs[2]	7.80	1.09	1.13	14.8	6.18	1.54	0.92	23.6
Na	3,810	417	3.44	6,944	2,947	480	286	4,844
K	573	74.7	0.60	1,076	188	35.1	105	440
Zn	520	174	0.00	1,846	100	46.3	14.1	477
V	2.58	0.39	0.00	4.85	10.2	2.16	0.90	28.6
Pb	40.7	11.2	0.02	108	5.68	1.36	1.74	16.3

Ni	2.64	0.51	0.00	6.43	5.31	1.07	1.57	16.6
Mn	20.1	3.29	0.02	37.9	4.37	1.35	1.37	17.1
Cd	2.16	1.45	0.00	22.1	0.17	0.06	0.06	0.84
ΣElements[3]	6,283	714	5.42	11,278	4,002	609	829	7,598

[1] ΣTotal carbon was the sum of OC and EC.

[2] ΣWSIs was the sum of three anions and five cations.

[3] ΣElements was the sum of 23 elements including the 8 selected elements.

[4] 95%CI represents the 95% confidence interval.

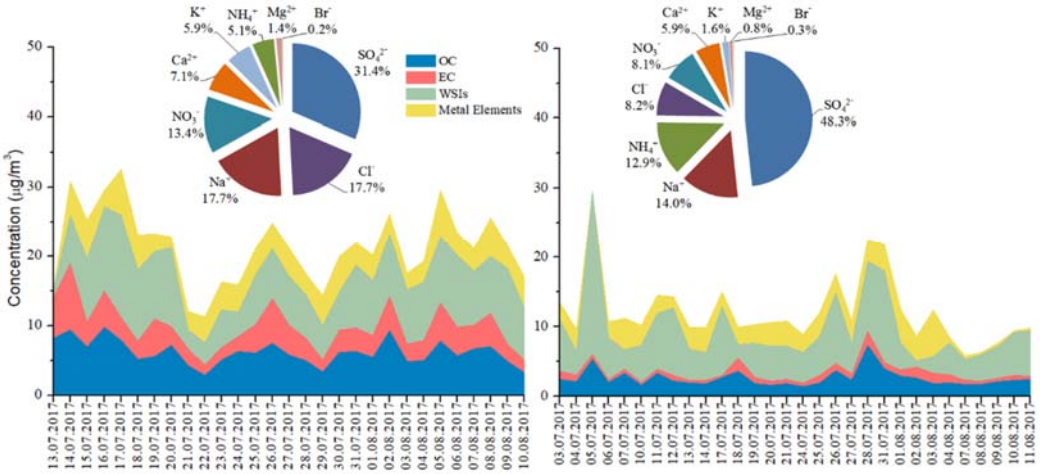

Fig. 3 Daily variations of OC, EC, WSIs and elements in $PM_{2.5}$ at ULG (left) and TC (right). Concentrations of duplicated elements (*i.e.* Na, K, Ca, Mg) were excluded from the sum of metal elements. Pie charts represent the composition of WSIs.

3.2. Chemical signatures of $PM_{2.5}$

3.2.1. Carbonaceous species

Carbonaceous aerosol (total carbon) consists of two main components, *i.e.* EC and OC. EC directly originates from primary combustion, whereas OC is either emitted from primary sources or produced by chemical reactions among gaseous precursors (So et al., 2007; Fu et al., 2014; Wang et al., 2018). At ULG, the good correlation between OC and EC (R^2=0.79, p<0.01) implied that both OC and EC were highly associated with similar primary emissions, probably attributed to traffic activities and industrial combustion processes. At TC, however, the weak correlation between OC and EC (R^2=0.48, p<0.01) indicated their different sources. It was well known that formation of secondary organic carbon (SOC) increased the OC/EC ratio by enhancing the OC level, and the OC/EC ratio > 2 was generally the sign of SOC generation (Chow et al.,

1996; Niu et al., 2013). In this study, the average OC/EC ratio was 1.81±0.18 at ULG and 3.51±0.60 at TC, suggesting the dominance of primary emissions at ULG and SOC formation at TC. In addition, by looking into the day-to-day variations, it was found that there were 25 days with OC/EC > 2 at TC, while only 6 days at ULG, confirming more predominant SOC formation at TC. To further investigate the primary and secondary sources, OC was divided into primary organic carbon (POC) and secondary organic carbon (SOC), following the equations below (Huang et al., 2012):

$$POC = EC \times (OC/EC)_{min} \quad (5)$$

$$SOC = OC - POC \quad (6)$$

where $(OC/EC)_{min}$ was the arithmetic mean of the three minimum OC/EC ratios of the sample dataset (the days with average OC/EC ratio > 2, when secondary OC was likely formed, were picked out for calculation). The $(OC/EC)_{min}$ was determined for each site (1.07 for ULG and 1.49 for TC). The average concentrations of POC and SOC were 5.45±0.79 μg/m^3 and 0.72±0.54 μg/m^3 at ULG, explaining 88±8% and 12±8% of the total OC, respectively, while they were 1.28±0.25 μg/m^3 and 1.30±0.41 μg/m^3 at TC, accounting for 53±9% and 47±9% of overall OC (Table 2). The higher proportion of SOC at TC suggested more intensive secondary formation than at ULG.

Table 2 Average values of POC, SOC, POC/OC and SOC/OC ratios at ULG and TC. The units of POC and SOC are μg/m^3.

	ULG				TC			
	Average	95% CI	Min.	Max.	Average	95%CI	Min.	Max.
POC	5.45	0.79	1.78	9.75	1.28	0.25	0.57	3.59
SOC	0.72	0.54	0.00	4.47	1.30	0.41	0.00	4.47
POC/OC	0.88	0.08	0.38	1.00	0.53	0.09	0.17	1.00
SOC/OC	0.12	0.08	0.00	0.62	0.47	0.09	0.00	0.83

The daily variations of POC, SOC and SOC/OC are displayed in Fig. 4. Note: only the days with OC/EC > 2 were selected. At TC, higher SOC values were observed on July 5 and 28 , along with SOC/OC ratio of 0.83 and 0.61, respectively. In addition, very high SOC/OC ratio (0.78) was found on July 17. In general, high temperature and solar radiation promote the SOC formation (Huang et al., 2012), while high relative humidity causes the attachment of more SOC tracers (SVOC) on particulate matter (Han et al.,

2011). During the sampling campaign, the average temperature, solar radiation, relative humidity and O_3 mixing ratio were 29.4°C, 241w/m^3, 81.9% and 14.73 ppbv at TC, respectively. Compared with the averages, significantly higher relative humidity was found on July 5 (84%) and July 17 (90%) (p<0.05), and the highest solar radiation (509 w/m^3) and higher O_3 (30.4 ppbv) levels were observed on July 28 (p<0.05), which were favorable for the photochemical SOC formation. At ULG, there appeared no extremely high SOC/OC ratio (maximum ratio < 0.62) during the whole sampling campaign. It is noteworthy that although the average POC dominated the OC concentration at ULG for the whole sampling period, the SOC values ranged from 1.64 to 4.47 μg/m^3 on the selected 6 days, much higher than the SOC levels on most days at TC and on the remaining days at ULG, indicating that much more secondary formation occurred on these 6 days at ULG. However, on most of the sampling days, the primary emissions were far more than the secondary formation at ULG. Since the average relative humidity and solar radiation on these 6 days were similar to the rest days with low OC/EC ratios at ULG, the exact reasons of high SOC formation on these 6 days remained uncertain.

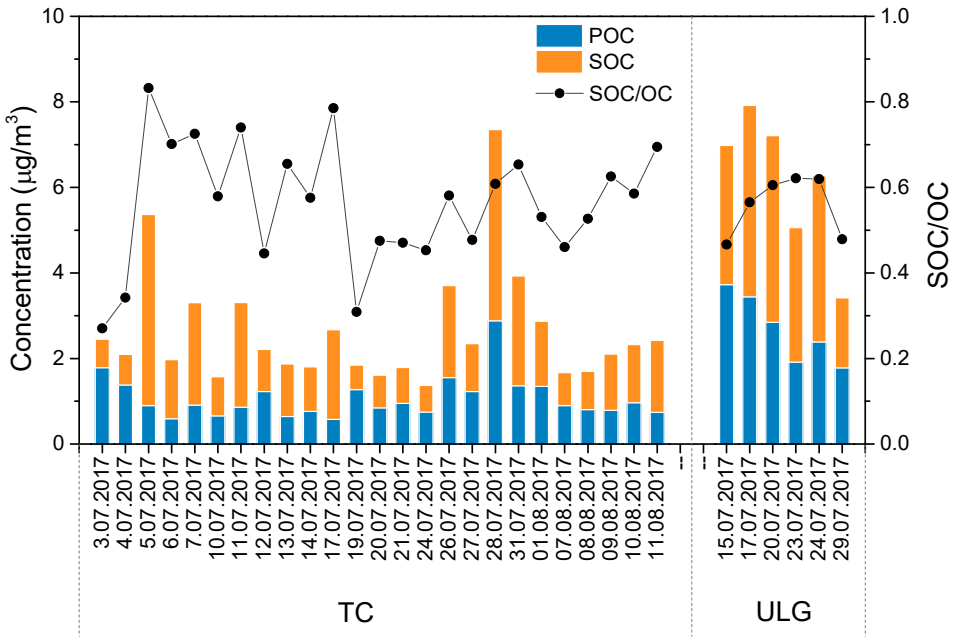

Fig. 4 Daily variations of POC, SOC and SOC/OC at TC and ULG. Sampling days with OC/EC > 2 were selected.

3.2.2. Water soluble ions

Fig. 5 shows the correlations of (a) Mg^{2+} vs. Na^{+}; (b) Cl^{-} vs. Na^{+}; (c) NH_4^{+} vs. SO_4^{2-} and (d) (NH_4^{+} + Na^{+}) vs. SO_4^{2-}. Please note: concentration of WSIs here was equivalent concentrations ($\mu eq/m^3$). Typically, ratios of Mg^{2+}/Na^{+} and Cl^{-}/Na^{+} were about 0.23 and 1.17 in the seawater, respectively (Chester, 1990). If the Mg^{2+}/Na^{+} and Cl^{-}/Na^{+} ratios were higher than 0.23 and 1.17, non-sea salt sources dominated. In contrast, lower ratios indicated the abundance of sea salt-related substances (Zhang et al., 2014). In this study, the slopes of Mg^{2+}/Na^{+} derived from linear regression were 0.16 (R^2=0.87) at ULG and 0.17 (R^2=0.82) at TC, much lower than 0.23 (Fig. 5a). Furthermore, the slopes of Cl^{-}/Na^{+} were 0.83 (R^2=0.66) at ULG and 0.82 (R^2=0.83) at TC, lower than 1.17 (Fig. 5b). Similar ratios of Mg^{2+}/Na^{+} and Cl^{-}/Na^{+} were found between ULG and TC. Ratios lower than reference values indicated the dominance of sea salt-related substances. In addition, Mg^{2+}/Na^{+} ratios at two sites suggested a removal of Mg^{2+}, which was possibly attributable to its combination with dissociated OH-group in seawater at relatively high temperatures. Moreover, lower Cl^{-}/Na^{+} in this study indicated the loss of Cl^{-}, which occurred during aging of sea salt when Cl^{-} was driven off by reaction of NaCl with acids such as HNO_3 (from NO_2 oxidation) and H_2SO_4 (from SO_2 oxidation). For the sake of completeness, pearson correlation analyses on individual anions and cations at ULG and TC are provided in Tables S1 and S2. Fig. 5c illustrates the correlation of NH_4^{+} with SO_4^{2-}. The slopes were 0.41 (R^2 =0.31) at ULG and 0.62 (R^2=0.62) at TC, suggested the existence of ammonium bisulfate (NH_4HSO_4) or excess SO_4^{2-} (Ianniello et al., 2011). We further considered the sum of NH_4^{+} and Na^{+} in this charge balance analysis (Fig. 5d). The higher slope (> 1) at ULG indicated that SO_4^{2-} was almost neutralized by NH_4^{+} and Na^{+}, whereas the lower slope (< 1) at TC suggested the lack of NH_4^{+} and Na^{+} for neutralizing with SO_4^{2-} and presented as NH_4HSO_4 and $NaHSO_4$. Furthermore, the good correlations of NO_3^{-} with Na^{+}, Mg^{2+} and Ca^{2+} found at TC (Table S2), implied that NO_3^{-} existed in the form of $NaNO_3$, $Mg(NO_3)_2$ and $Ca(NO_3)_2$. Overall, the ratios and correlations of Na^{+}, Mg^{2+}, Cl^{-}, $NO_3^{-}$and SO_4^{2-} suggested the aged sea salt source of $PM_{2.5}$ at ULG and TC.

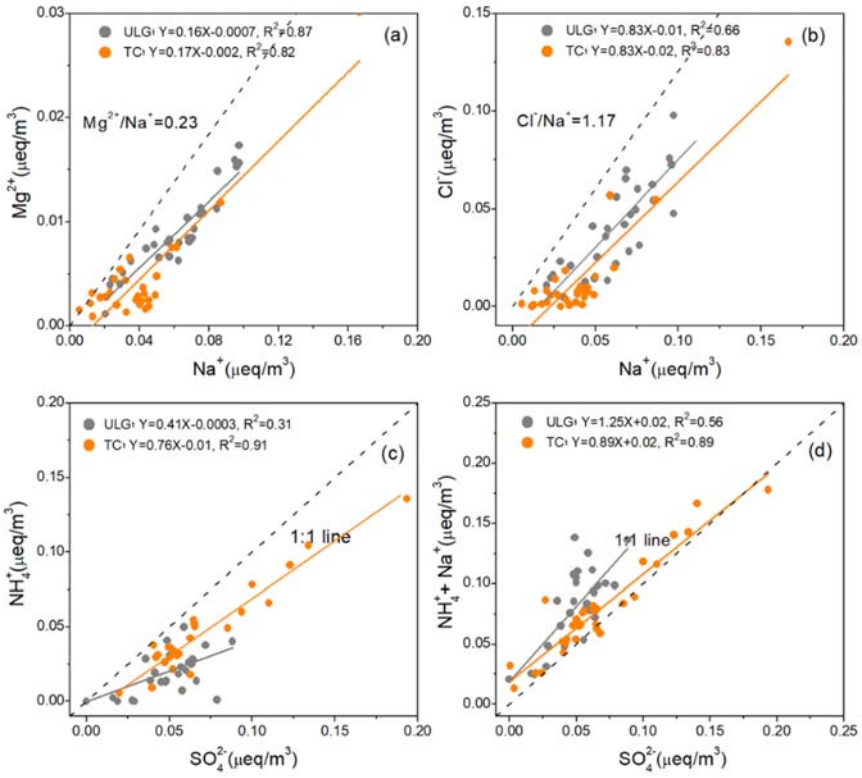

386

387 **Fig. 5** Correlations between cations and anions at TC and ULG: (a) Mg^{2+} versus Na^{+};
388 (b) Cl^{-} versus Na^{+}; (c) NH_4^{+} versus SO_4^{2-} and (d) (NH_4^{+} + Na^{+}) versus SO_4^{2-}. (Dashed
389 lines in (a) and (b) represents Mg^{2+}/Na^{+} and Cl^{-}/Na^{+} ratios found in sea water referred
390 to Chester, 1990)

391 ***3.2.3. Elements***

392 Enrichment factor (EF) analysis was adopted to facilitate the classification of natural
393 and anthropogenic sources (Rogula-Kozłowska et al., 2013; Luo et al., 2018). The EF
394 was calculated based on the following equation:

395 $$EF_X = \frac{(C_X/C_R)_{Aerosol}}{(C_X/C_R)_{Crust}} \quad (7)$$

396 where $(C_X/C_R)_{Aerosol}$ was the mass concentration ratio of element X versus reference
397 element R in the aerosol, while $(C_X/C_R)_{Crust}$ denoted the mass concentration ratio of X
398 to R in crust. In this study, the observed Al was chosen as the reference element. The
399 concentrations of elements in crust referred to the levels in the Earth's soil (Alekseenko
400 and Alekseenko, 2014) at ULG and the levels in the Chinese topsoil (Wei et al., 1991)
401 at TC. The EF values of elements in $PM_{2.5}$ at ULG and TC are shown in Fig. 6.

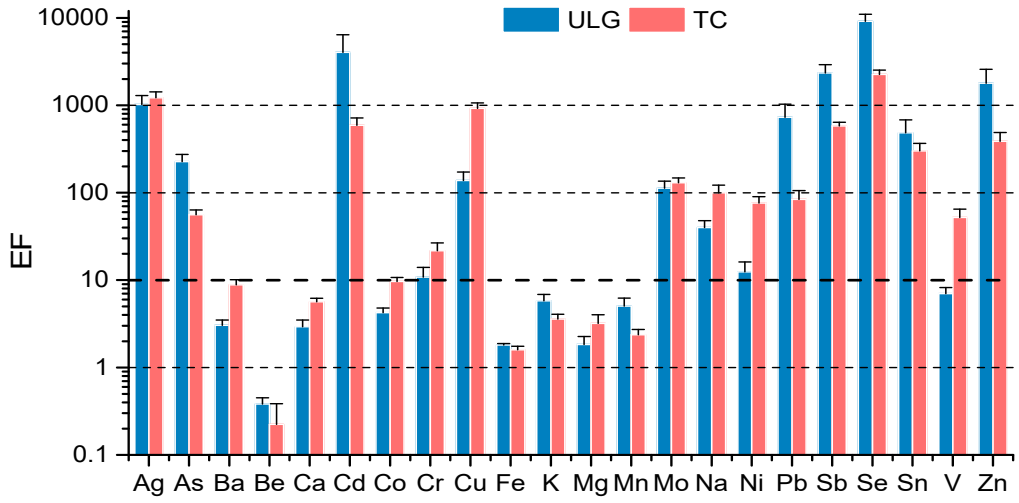

Fig. 6 EF analysis for the elements in $PM_{2.5}$ at ULG and TC. Error bars represents 95% CI for each group of data.

Extremely high EF values (>1000) were found for Cd, Sb, Se and Zn at ULG, meanwhile their values were also around 1000 at TC, suggesting severe anthropogenic pollution in both regions (Zhang et al., 2015). Cd was a highly toxic heavy metal in biological systems, which was a constituent of effluents from paint industries in Lagos (Bawa-Allah et al., 2018), while Sb and Se were emitted from vehicles (Owoade et al., 2013; Lyu et al., 2016). Furthermore, Zn had good correlation with Pb (R^2=0.90, Fig. S4) at ULG, which were identified as the significant tracers of industries in Lagos (Owoade et al., 2009), while Zn was identified as the tracer of mobile sources in Hong Kong (Guo et al., 2009a). Moreover, the levels of Cd, Zn and Pb at ULG were much higher than those observed at TC (all p<0.05) (Table 1), indicating more severe pollution caused by industries at ULG. In addition, elements such as Ag, As, Cu, Mo and Sn with high EF values at both sites further demonstrated the importance of anthropogenic sources to the $PM_{2.5}$ pollution. However, the EF values of V and Ni were only about 10 at ULG but close to 90 at TC, suggesting that the source strength of V and Ni at TC was higher than at ULG. It was well known that V and Ni were typical tracers of ship emissions (Cheng et al., 2015). Besides, much higher correlation between Al and Fe was found at ULG than at TC (Fig. S4), and they were both originated from soil dust (Huang et al., 2014; Orogade et al., 2016).

3.3. Source identification and apportionment

Fig. 7 and Fig. 8 show the six source profiles in percentages resolved from PMF at ULG

425 and TC. Factor profiles in concentration for each species are presented in Table S3 and
426 S4.

427 Factor 1 was distinguished by the high proportions of OC, EC, As and Se at ULG and
428 TC, as well as considerable Zn, Pb, Cu, Al, Fe and Cd at TC, suggesting the vehicular
429 emissions and road erosion at both sites (Guo et al., 2009a; Huang et al., 2014; Cheng
430 et al., 2015). Pb-containing fossil fuel has been banned in Hong Kong since 1999
431 (HKEPD, 2002). Looking into wind speed/direction on high-Pb days (Fig. S3), only
432 three days (July 12, 14 and 27) were accompanied with northerly wind, indicating
433 partially regional transport, while southwest winds dominated on another two days
434 (July 31 and Aug. 1) suggesting no air masses from inland China. Therefore, the
435 appreciable Pb found at TC might be likely attributable to the on-use of Pb-containing
436 materials in vehicles, road dust resuspension (Song et al., 2016; Adeniran et al., 2017)
437 or regional transport.

438 Factor 2 had high fractions of Na^+, Mg^{2+} and Cl^-, representing sea salt source. The
439 existence of NO_3^- and SO_4^{2-} in this factor at both sites indicated the aging of sea salt,
440 through the reaction between NaCl and acids like HNO_3 and H_2SO_4 (Gianguzza et al.,
441 2002), which was in accordance with the result in section 3.2.2. Higher percentage of
442 NO_3^- in this factor relative to Cl^- at ULG might imply more aged sea salt in Lagos.

443 Factor 3 at TC was dominated by NH_4^+ and SO_4^{2-}, implying the source of secondary
444 sulfate (Huang et al., 2014). In addition, K^+ had high loading in this factor. Earlier
445 studies found that regional transport made significant contribution to sulfate at TC
446 (Louie et al., 2005). Besides, the good correlation of K^+ with SO_4^{2-} in this factor
447 suggested that K^+ was likely from the neighbouring Pearl River Delta (PRD) region
448 because biomass burning was prohibited in Hong Kong. Similarly, Factor 3 at ULG was
449 mainly distinguished by NH_4^+, SO_4^2, NO_3^- along with K^+, indicating a combination of
450 both Secondary Inorganic Aerosol (SIA) and biomass burning (Owoade et al., 2013).
451 The high percentage of K^+ in Factor 3 in Lagos was caused by biomass burning, which
452 was further confirmed by the numerous wildfire spots observed via satellite during the
453 sampling period (Fig. S5).

454 Factor 4 was classified as fugitive dust because of high loadings of Al and Fe. These
455 elements were primarily originated from crustal substances (Guo et al., 2009a).

Factor 5 at ULG was recognized as the source related to industrial processes due to the high percentages of Cd, Zn and Pb, as well as partial Cu and Ni. In Lagos, Cd was mainly emitted from paint industries, while Zn and Pb were related to the scrap and additives used in the electric-arc furnace section in iron and steel smelting industry (Owoade et al., 2009). Since no measurable EC and OC were found in this factor, we classified it as industrial-related emissions rather than vehicular emissions. At TC, however, Factor 5 was dominated by NO_3^-, so it was characterized as secondary nitrate. The separation of secondary NO_3^- from factor 3 at TC might be attributable to different formation mechanism of NO_3^- and SO_4^{2-} or the interference of regional transport.

Factor 6 at both sites was characterized by remarkable percentages of Ni and V, which were good tracers for heavy/residual oil combustion (Corbett and Fischbeck, 1997). Lagos is one of the largest seaports in Africa, and Hong Kong is a top-10 harbour city in the world, therefore, this factor was identified as ship emissions. It is noteworthy that high loading of Cu collocated with Ni and V at ULG might be related to ship emissions and/or cargo vehicles at the port (Orogade et al., 2016), while high proportions of NH_4^+ and SO_4^{2-} in Factor 6 at TC could be associated with in-situ secondary formation.

Table 3 presents the source concentrations and contributions to $PM_{2.5}$ at ULG and TC. Vehicular emissions made the largest contribution at ULG, accounting for 5.75±0.56 μg/m^3 (32.2±3.18%), followed by sea salt (3.70±0.62 μg/m^3, 20.7±2.46%), SIAs as well as biomass burning (3.42±0.65 μg/m^3, 19.2±3.65%), ship emission (2.49±0.62 μg/m^3, 13.9±2.52%). The fugitive dust only contributed 1.54±0.11 μg/m^3, 8.65±2.43%) at ULG, when industry processes explained 0.96±0.44 μg/m^3 (5.36±1.51%). At TC, the secondary sulfate together with the regionally transported biomass burning accounted for the highest proportion of total $PM_{2.5}$ (2.19±0.41 μg/m^3, 24.6±3.67%), so did the ship emission (2.11±0.39 μg/m^3, 23.7±2.34%). In addition, sea salt contributed 1.31±0.38 μg/m^3, (14.7±2.34%), followed by fugitive dust (1.20±0.22 μg/m^3, 13.4±1.73%). Moreover, secondary nitrate (1.06±0.24 μg/m^3, 11.9±1.69%) made similar contribution as vehicular emission (1.05±0.30 μg/m^3, 11.8±2.62%).

Comparing the sources contributing to $PM_{2.5}$ at ULG and TC, vehicular emission was the top contributor at ULG while SIAs with biomass burning made the largest contribution at TC, reflecting that control strategies on primary emissions in Hong Kong achieved remarkable effects. For those duplicated $PM_{2.5}$ sources, generally,

significantly higher concentrations were found at ULG (p<0.05), except for the comparable levels in SIAs (including sulfate and nitrate) with biomass burning at two sites (3.42±0.65 μg/m^3 at ULG, 3.25±0.42 μg/m^3 at TC). The sum of vehicular emission and fugitive dust (7.29±0.60 μg/m^3) at ULG was triple that at TC (2.25±0.50 μg/m^3) (p<0.01), confirming the severe street-level air pollution in Lagos (Komolafe et al., 2014), which might be caused by the combustion of unqualified fuel as well as construction activities that were not strictly controlled. Bearing the situation in mind, effective control measures in Hong Kong were worth learning from. For example, the Hong Kong government promoted cleaner alternatives to diesel vehicles. For the remaining diesel vehicles, not only fuel was upgraded periodically, but also particulate traps and catalytic converters were added for retrofit. Moreover, industrial processes source related to iron and steel smelting as well as paints industries was found at ULG, whereas there was no such industry in Hong Kong.

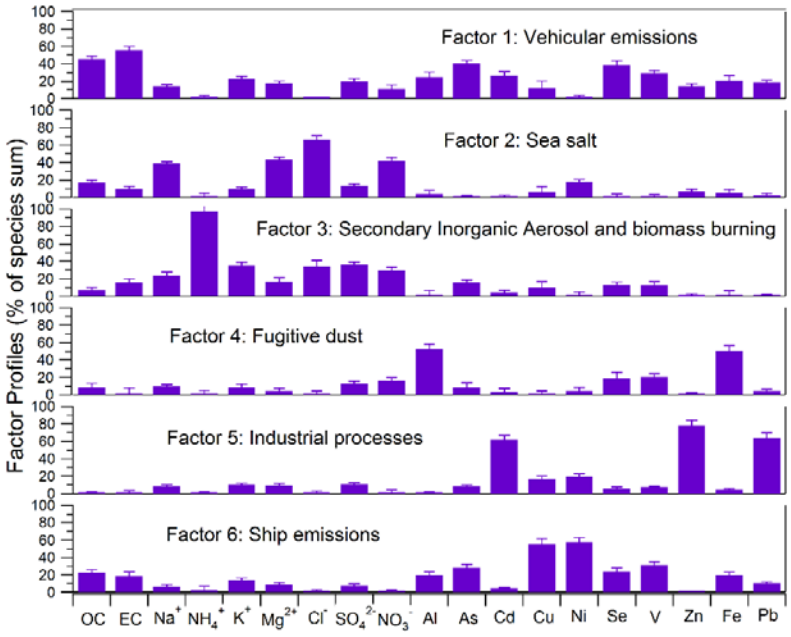

Fig. 7 Source profiles of $PM_{2.5}$ at ULG. Error bars represent 95% CI estimated by bootstrap method in PMF.

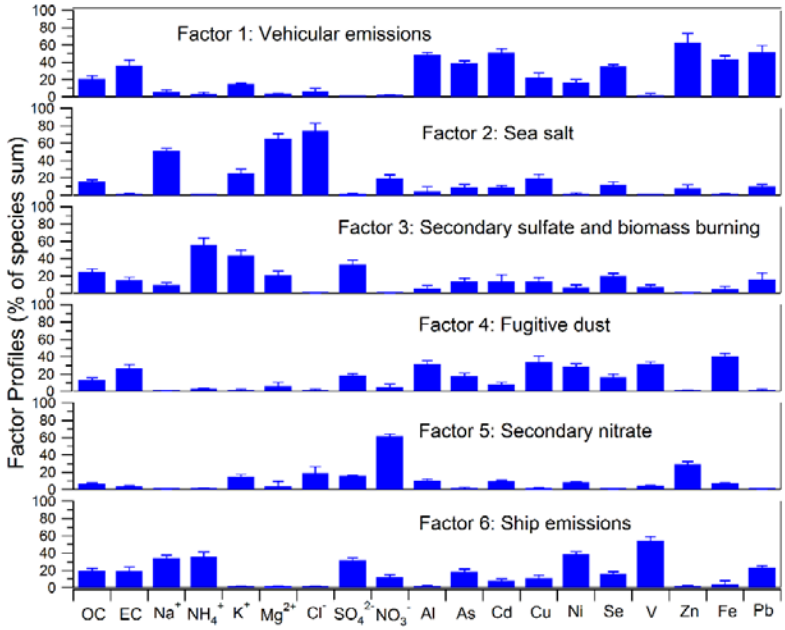

Fig. 8 Source profiles of $PM_{2.5}$ at TC. Error bars represent 95% CI estimated by bootstrap method in PMF.

Table 3 Average source concentrations (μg/m^3) and contribution percentages (%) at ULG and TC. Error bars represent 95% CI estimated by bootstrap method in PMF.

Source	ULG		TC	
	Concentration	Percentage	Concentration	Percentage
Vehicular emissions	5.75±0.56	32.2±3.18	1.05±0.30	11.8±2.62
Sea salt	3.70±0.62	20.7±2.46	1.31±0.38	14.7±2.34
SIAs and biomass burning	3.42±0.65	19.2±3.65		
Secondary sulfate and biomass burning			2.19±0.41	24.6±3.67
Secondary nitrate			1.06±0.24	11.9±1.69
Fugitive dust	1.54±0.11	8.65±2.43	1.20±0.22	13.4±1.73
Ship emissions	2.49±0.62	13.9±2.52	2.11±0.39	23.7±2.34
Industrial processes	0.96±0.44	5.36±1.51		

4. Conclusions

Intensive sampling campaigns were simultaneously carried out from July to August in 2017 in Lagos, Nigeria and Hong Kong, China, in order to obtain detailed chemical characteristics of $PM_{2.5}$ pollution in these two regions. The levels of carbonaceous species (p<0.001) and elements (p<0.05) at ULG were higher than those

517 at TC, suggesting more severe particulate pollution in Lagos, while levels of WSIs were
518 comparable at two sites (p=0.05). It was found that carbonaceous species was the most
519 abundant components in $PM_{2.5}$ at ULG, while the most predominant compounds in
520 $PM_{2.5}$ at TC were WSIs especially SO_4^{2-}. A good correlation between EC and OC
521 (R^2=0.79, p<0.01) at ULG suggested their primary emission sources, likely related to
522 local vehicular emissions and industrial combustion processes, however, the weak
523 correlation at TC (R^2=0.48, p<0.01) revealed their secondary sources. By investigating
524 ratios of SOC/OC, higher percentages of OC were contributed by SOC in Hong Kong.
525 Furthermore, Cl^-/Na^+ ratios indicated the aging of sea salt at two sites.

526 $PM_{2.5}$ sources were resolved by the PMF model at both ULG and TC, including sea salt,
527 vehicular emissions, ship emissions, fugitive dust, iron and steel smelting industry, and
528 SIAs (secondary sulfate and secondary nitrate)/biomass burning. The largest
529 contributor to $PM_{2.5}$ was vehicular emissions (32.2%) at ULG, while SIAs, including
530 secondary sulfate and nitrate, together with biomass burning (36.5%) made the most
531 significant contribution at TC. Furthermore, industrial processes source was unique at
532 ULG. In the inter-comparison, levels of four duplicated primary sources were much
533 higher (p<0.05) at ULG, while levels of SIA/biomass burning was comparable at two
534 sites. The sum of vehicular emission and fugitive dust at ULG was triple that at TC
535 (p<0.01). The findings provided the first-hand $PM_{2.5}$ data in Lagos, which
536 would be helpful for local government to formulate and implement effective control
537 measures on $PM_{2.5}$ via sharing the experience of Hong Kong.

538 **Acknowledgements**

539 This study was supported by the National Key R&D Program of China via grant No.
540 2017YFC0212001, Research Grants Council of the Hong Kong Special Administrative
541 Region Government via grants PolyU 152052/14E, PolyU 152052/16E and
542 CRF/C5004-15E, the Public Policy Research Funding Scheme from Policy Innovation
543 and Co-ordination Office of the Hong Kong Special Administrative Region
544 Government (Project Number: 2017.A6.094.17D), and the Environment and
545 Conservation Fund (ECF Project 59/2015).

546

547

548 **References**

549 Adelekan, I.O., 2009. Vulnerability of poor urban coastal communities to climate change in
550 Lagos, Nigeria. Fifth Urban research symposium, pp. 28-30.
551 Alekseenko, V., Alekseenko, A., 2014. The abundances of chemical elements in urban soils.
552 Journal of Geochemical Exploration 147, 245-249.
553 Adeniran, J. A., Yusuf, R. O., Olajire, A. A., 2017. Exposure to coarse and fine particulate matter
554 at and around major intra-urban traffic intersections of Ilorin metropolis, Nigeria. Atmospheric
555 Environment, 166, 383-392.
556 Anton, W., Wolfram, B., Catrin, A., Bryan, H., Erich, J., Gabriele, W., Harrison, R.M., Schins,
557 R.P.F., 2010. Oxidant generation and toxicity of size-fractionated ambient particles in human
558 lung epithelial cells. Environmental Science & Technology 44, 3539-3545.
559 Antonel, J., Chowdhury, Z., 2014. Measuring ambient particulate matter in three cities in
560 Cameroon, Africa. Atmospheric Environment 95, 344-354.
561 AUDEE, 2018. National standards for criteria air pollutants 1 in Australia. Avaliable from:
562 http://www.environment.gov.au/protection/publications/factsheet-national-standards-criteria-
563 air-pollutants-australia.
564 Bawa-Allah, K., Saliu, J., Otitoloju, A., 2018. Heavy Metal Pollution Monitoring in Vulnerable
565 Ecosystems: A Case Study of the Lagos Lagoon, Nigeria. Bulletin of environmental
566 contamination and toxicology 100, 609-613.
567 Cheng, Y., Lee, S.C., Gu, Z.L., Ho, K.F., Zhang, Y.W., Huang, Y., Chow, J.C., Watson, J.G.,
568 Cao, J.J., Zhang, R.J., 2015. PM2.5 and PM10-2.5 chemical composition and source
569 apportionment near a Hong Kong roadway. Particuology 18, 96-104.
570 Chester, R., 1990. Marine Geochemistry. Cambridge University Press, London, 698pp.
571 Cheung, H.C., Tao, W., Baumann, K., Hai, G., 2005. Influence of regional pollution outflow on
572 the concentrations of fine particulate matter and visibility in the coastal area of southern China.
573 Atmospheric Environment 39, 6463-6474.
574 Chow, J.C., Watson, J.G., Lu, Z., Lowenthal, D.H., Frazier, C.A., Solomon, P.A., Thuillier, R.H.,
575 Magliano, K., 1996. Descriptive analysis of PM 2.5 and PM 10 at regionally representative
576 locations during SJVAQS/AUSPEX. Atmospheric Environment 30, 2079-2112.
577 Cooke, R.M., Wilson, A.M., Tuomisto, J.T., Morales, O., Tainio, M., Evans, J.S., 2007. A
578 Probabilistic characterization of the relationship between fine particulate matter and mortality:
579 Elicitation of European experts. Environmental Science & Technology 41, 6598-6605.
580 Corbett, J.J., Fischbeck, P., 1997. Emissions from ships. Science 278, 823-824.
581 Crouse, D.L., Peters, P.A., van Donkelaar, A., Goldberg, M.S., Villeneuve, P.J., Brion, O., Khan,
582 S., Atari, D.O., Jerrett, M., Pope, C.A., Brauer, M., Brook, J.R., Martin, R.V., Stieb, D., Burnett,
583 R.T., 2012. Risk of Non accidental and Cardiovascular Mortality in Relation to Long-term
584 Exposure to Low Concentrations of Fine Particulate Matter: A Canadian National-Level Cohort
585 Study. Environmental Health Perspectives 120, 708-714.
586 EEA, 2017. Air quality standards. Avaliable from: https://www.eea.europa.eu/themes/air/air-
587 quality-standards.
588 Ferguson, R., Wilkinson, W., Hill, R., 2000. Electricity use and economic development. Energy
589 policy 28, 923-934.
590 Fiore, A.M., Vaishali, N., Spracklen, D.V., Allison, S., Nadine, U., Michael, P., Dan, B.,
591 Cameron-Smith, P.J., Irene, C., Collins, W.J., 2012. Global air quality and climate. Chemical
592 Society Reviews 41, 6663-6683.
593 Fu, X., Wang, X., Guo, H., Cheung, K., Ding, X., Zhao, X., He, Q., Gao, B., Zhang, Z., Liu, T.,
594 2014. Trends of ambient fine particles and major chemical components in the Pearl River Delta
595 region: observation at a regional background site in fall and winter. Science of the Total
596 Environment 497-498, 274-281.
597 Gianguzza, A., Pelizzetti, E., Sammartano, S., Biochemie, Meereskunde, 2002. Chemistry of
598 Marine Water and Sediments. Environmental Science 83, 625-626.
599 GovHK, 2019. Hong Kong Overview. Avaliable from:
600 https://www.gov.hk/tc/about/abouthk/facts.htm.
601 Gumede, P.R., Savage, M.J., 2017. Respiratory health effects associated with indoor particulate
602 matter (PM2.5) in children residing near a landfill site in Durban, South Africa. Air Quality
603 Atmosphere and Health 10, 853-860.

Guo, H., Ding, A.J., So, K.L., Ayoko, G., Li, Y.S., Hung, W.T., 2009a. Receptor modeling of source apportionment of Hong Kong aerosols and the implication of urban and regional contribution. Atmospheric Environment 43, 1159-1169.
Guo, H., Jiang, F., Cheng, H., Simpson, I., Wang, X., Ding, A., Wang, T., Saunders, S., Wang, T., Lam, S., 2009b. Concurrent observations of air pollutants at two sites in the Pearl River Delta and the implication of regional transport. Atmospheric Chemistry and Physics 9, 7343-7360.
Han, Y.J., Kim, S.R., Jung, J.H., 2011. Long-term measurements of atmospheric PM 2.5 and its chemical composition in rural Korea. Journal of Atmospheric Chemistry 68, 281-298.
HKEPD, 2002. Ban on leaded petrol gazetted. Avaliable from: https://www.epd.gov.hk/epd/english/news_events/press/press_990205.html.
Henry, R. C., Lewis, C. W., Hopke, P. K., Williamson, H. J., 1984. Review of receptor model fundamentals. Atmospheric Environment (1967) 18(8), 1507–1515.
Ho, K.F., Lee, S.C., Cao, J.J., Chow, J.C., Watson, J.G., Chan, C.K., 2006. Seasonal variations and mass closure analysis of particulate matter in Hong Kong. Science of the Total Environment 355, 276-287.
Hu, D., Bian, Q., Lau, A. K., Yu, J. Z., 2010. Source apportioning of primary and secondary organic carbon in summer PM2.5 in Hong Kong using positive matrix factorization of secondary and primary organic tracer data. Journal of Geophysical Research: Atmospheres 115(D16).
Huang, H., Ho, K.F., Lee, S.C., Tsang, P.K., Ho, S.S.H., Zou, C.W., Zou, S.C., Cao, J.J., Xu, H.M., 2012. Characteristics of carbonaceous aerosol in PM 2.5 : Pearl Delta River Region, China. Atmospheric Research 104-105, 227-236.
Huang, X.H.H., Bian, Q.J., Ng, W.M., Louie, P.K.K., Yu, J.Z., 2014. Characterization of PM2.5 Major Components and Source Investigation in Suburban Hong Kong: A One Year Monitoring Study. Aerosol and Air Quality Research 14, 237-250.
Ianniello, A., Spataro, F., Esposito, G., Allegrini, I., Hu, M., Zhu, T., 2011. Chemical characteristics of inorganic ammonium salts in PM 2.5 in the atmosphere of Beijing (China). Atmospheric Chemistry and Physics 11, 10803-10822.
Kerminen, V.M., Teinilä, K., Hillamo, R., 2000. Chemistry of sea-salt particles in the summer Antarctic atmosphere. Atmospheric Environment 34, 2817-2825.
Kim, B. M., Cassmassi, J., Hogo, H., Zeldin, M. D., 2001. Positive organic carbon artifacts on filter medium during PM2.5 sampling in the South Coast Air Basin. Aerosol Science & Technology 34(1), 35-41.
Komolafe, A. A., Adegboyega, S. A. A., Anifowose, A. Y., Akinluyi, F. O., Awoniran, D. R., 2014. Air pollution and climate change in Lagos, Nigeria: needs for proactive approaches to risk management and adaptation. American Journal of Environmental Sciences 10(4), 412.
Krall, J.R., Mulholland, J.A., Russell, A.G., Balachandran, S., Winquist, A., Tolbert, P.E., Waller, L.A., Sarnat, S.E., 2017. Associations between Source-Specific Fine Particulate Matter and Emergency Department Visits for Respiratory Disease in Four US Cities. Environmental Health Perspectives 125, 97-103.
Louie, P.K.K., Watson, J.G., Chow, J.C., Chen, A., Sin, D.W.M., Lau, A.K.H., 2005. Seasonal characteristics and regional transport of PM2.5 in Hong Kong. Atmospheric Environment 39, 1695-1710.
Luo, Y.Y., Zhou, X.H., Zhang, J.Z., Xiao, Y., Wang, Z., Zhou, Y., Wang, W.X., 2018. PM 2.5 pollution in a petrochemical industry city of northern China: Seasonal variation and source apportionment. Atmospheric Research.
Lyu, X.P., Chen, N., Guo, H., Zeng, L.W., Zhang, W.H., Shen, F., Quan, J.H., Wang, N., 2016. Chemical characteristics and causes of airborne particulate pollution in warm seasons in Wuhan, central China. Atmospheric Chemistry & Physics 16, 1-35.
Mader, B. T., Schauer, J. J., Seinfeld, J. H., Flagan, R. C., Yu, J. Z., Yang, H., Lim, H. J., Turpin, B. J., Deminter, J. T., Heidemann, G., Bae, M. S., Quinn, P., Bates, T., Eatough, D. J., Huebert, B. J., Bertram, T., Howell, S., 2003. Sampling methods used for the collection of particle-phase organic and elemental carbon during ACE-Asia. Atmospheric Environment 37(11), 1435-1449.
Makinde, T., 2005. Problems of policy implementation in developing nations: The Nigerian

659 experience. Journal of Social sciences 11, 63-69.
660 Niu, Z., Zhang, F., Chen, J., Yin, L., Wang, S., Xu, L., 2013. Carbonaceous species in PM 2.5
661 in the coastal urban agglomeration in the Western Taiwan Strait Region, China. Atmospheric
662 Research 122, 102-110.
663 Offor, I.F., Adie, G.U., Ana, G.R., 2016. Review of Particulate Matter and Elemental
664 Composition of Aerosols at Selected Locations in Nigeria from 1985–2015. Journal of Health
665 and Pollution 6, 1-18.
666 Olowoporoku, D., 2007. Air Quality Management in Lagos. Air Quality Management Resource
667 Centre, UWE, Bristol 9.
668 Orogade, S.A., Owoade, K.O., Hopke, P.K., Adie, D.B., Ismail, A., Okuofu, C.A., 2016. Source
669 Apportionment of Fine and Coarse Particulate Matter in Industrial Areas of Kaduna, Northern
670 Nigeria. Aerosol and Air Quality Research 16, 1179-1190.
671 Owoade, O., Olise, F., Obioh, I., Olaniyi, H., Ferrero, L., Bolzacchini, E., 2009. EDXRF
672 elemental assay of airborne particulates: A case study of an iron and steel smelting industry,
673 Lagos, Nigeria. Scientific Research and Essays 4, 1342-1347.
674 Owoade, O.K., Fawole, O.G., Olise, F.S., Ogundele, L.T., Olaniyi, H.B., Almeida, M.S., Ho,
675 M.-D., Hopke, P.K., 2013. Characterization and source identification of airborne particulate
676 loadings at receptor site-classes of Lagos Mega-City, Nigeria. Journal of the Air & Waste
677 Management Association 63, 1026-1035.
678 Park, S. S., Bae, M. S., Schauer, J. J., Kim, Y. J., Cho, S. Y., Kim, S. J., 2006. Molecular
679 composition of PM2. 5 organic aerosol measured at an urban site of Korea during the ACE-
680 Asia campaign. Atmospheric Environment 40(22), 4182-4198.
681 Petkova, E.P., Jack, D.W., Volavka-Close, N.H., Kinney, P.L., 2013. Particulate matter pollution
682 in African cities. Air Quality Atmosphere & Health 6, 603-614.
683 PRCMEE, 2018. GB 3095-2012. Avaliable from:
684 http://kjs.mee.gov.cn/hjbhbz/bzwb/dqhjbh/dqhjzlbz/201203/W020120410330232398521.pdf.
685 Rogula-Kozłowska, W., Błaszczak, B., Szopa, S., Klejnowski, K., Sówka, I., Zwoździak, A.,
686 Jabłońska, M., Mathews, B., 2013. PM 2.5 in the central part of Upper Silesia, Poland:
687 concentrations, elemental composition, and mobility of components. Environmental
688 monitoring and assessment 185, 581-601.
689 Samek, L., Stegowski, Z., Styszko, K., Furman, L., Fiedor, J., 2018. Seasonal contribution of
690 assessed sources to submicron and fine particulate matter in a Central European urban area.
691 Environmental Pollution 241, 406-411.
692 Seinfeld, J.H., Pandis, S.N., 1998. Atmospheric chemistry and physics : from air pollution to
693 climate change. Environment Science & Policy for Sustainable Development 40, 26-26.
694 So, K.L., Guo, H., Li, Y.S., 2007. Long-term variation of PM2.5 levels and composition at rural,
695 urban, and roadside sites in Hong Kong: Increasing impact of regional air pollution.
696 Atmospheric Environment 41, 9427-9434.
697 Song, C.B., He, J.J., Wu, L., Jin, T.S., Chen, X., Li, R.P., Ren, P.P., Zhang, L., Mao, H.J., 2017.
698 Health burden attributable to ambient PM2.5 in China. Environmental Pollution 223, 575-586.
699 Song, M., Yin, P., Zhao, L., Jiao, Z., Duan, S., Lu, G., 2016. Distribution and risk assessment
700 of heavy metals in sediments of the Pearl River Estuary, Southern China. Soil and Sediment
701 Contamination: An International Journal 25, 101-116.
702 Sonibare, J., Jimoda, L., 2009. Criteria Air Pollutants from Some Anthropogenic Combustion
703 Processes in Lagos, Nigeria. Energy Sources, Part A 31, 923-935.
704 USEPA, 2018. NAAQS Table. Avaliable from: https://www.epa.gov/criteria-air-
705 pollutants/naaqs-table.
706 Subramanian, R., Khlystov, A. Y., Cabada, J. C., Robinson, A. L., 2004. Positive and negative
707 artifacts in particulate organic carbon measurements with denuded and undenuded sampler
708 configurations special issue of aerosol science and technology on findings from the fine
709 particulate matter supersites program. Aerosol Science and Technology 38(S1), 27-48.
710 Wang, S.J., Zhou, C.S., Wang, Z.B., Feng, K.S., Hubacek, K., 2017. The characteristics and
711 drivers of fine particulate matter (PM2.5) distribution in China. Journal of Cleaner Production
712 142, 1800-1809.
713 Wang, W.F., Yua, J., Cui, Y., He, J., Xue, P., Cao, W., Ying, H.M., Gao, W.K., Yan, Y.C., Hu, B.,

714 Xin, J.Y., Wang, L.L., Liu, Z.R., Sun, Y., Ji, D.S., Wang, Y.S., 2018. Characteristics of fine
715 particulate matter and its sources in an industrialized coastal city, Ningbo, Yangtze River Delta,
716 China. Atmospheric Research 203, 105-117.
717 Wei, F.S., Chen, J.S., Wu, Y.Y., Zheng, C.J., 1991. Study of the background contents of 61
718 elements of soils in China. Environmental Science (in Chinese) 12, 12-19.
719 Yuan, Z.B., Yadav, V., Turner, J.R., Louie, P.K.K., Lau, A.K.H., 2013. Long-term trends of
720 ambient particulate matter emission source contributions and the accountability of control
721 strategies in Hong Kong over 1998-2008. Atmospheric Environment 76, 21-31.
722 Zhang, F., Wang, Z.W., Cheng, H.R., Lv, X.P., Gong, W., Wang, X.M., Zhang, G., 2015.
723 Seasonal variations and chemical characteristics of PM 2.5 in Wuhan, central China. Science
724 of the Total Environment 518-519, 97-105.
725 Zhang, R., Jing, J., Tao, J., Hsu, S.C., 2014. Chemical characterization and source
726 apportionment of PM2.5 in Beijing: seasonal perspective. Atmospheric Chemistry and
727 Physics,14,1(2014-01-08) 13, 7053-7074.
728 Zhou, Z., Dionisio, K.L., Verissimo, T.G., Kerr, A.S., Coull, B., Howie, S., Arku, R.E.,
729 Koutrakis, P., Spengler, J.D., Fornace, K., Hughes, A.F., Vallarino, J., Agyei-Mensah, S., Ezzati,
730 M., 2014. Chemical Characterization and Source Apportionment of Household Fine Particulate
731 Matter in Rural, Peri-urban, and Urban West Africa. Environmental Science & Technology 48,
732 1343-1351.